Ca^{2+} Channels from the Sea Urchin Sperm Plasma Membrane

A. LIÉVANO, E. C. VEGA-SAENZDEMIERA, and A. DARSZON

From the Departamento de Bioquimica, Centro de Investigación y de Estudios Avanzados del IPN, Apartado Postal 14-740, 07000 México, DF; and the Departamento de Ciencias Fisiológicas, Instituto de Ciencias, Universidad Autónoma de Puebla, Apartado Postal 406, Puebla, México

ABSTRACT Ca^{2+} influx across the sea urchin sperm plasma membrane is a necessary step during the egg jelly–induced acrosome reaction. There is pharmacological evidence for the involvement of Ca^{2+} channels in this influx, but their presence has not been directly demonstrated because of the small size of this cell. Sea urchin sperm Ca^{2+} channels are being studied by fusing isolated plasma membranes into planar lipid bilayers. With this strategy, a Ca^{2+} channel has been detected with the following characteristics: (*a*) the channel exhibits a high main-state conductance (γ_{MS}) of 172 pS in 50 mM $CaCl_2$ solutions with voltage-dependent decaying to smaller conductance states at negative E_m; (*b*) the channel is blocked by millimolar concentrations of Cd^{2+}, Co^{2+}, and La^{3+}, which also inhibit the egg jelly–induced acrosome reaction; (*c*) the γ_{MS} conductance sequence for the tested divalent cations is the following: $Ba^{2+} > Sr^{2+} > Ca^{2+}$; and (*d*) the channel discriminates poorly for divalent over monovalent cations ($P_{Ca}/P_{Na} = 5.9$). The sperm Ca^{2+} channel γ_{MS} rectifies in symmetrical 10 mM $CaCl_2$, having a maximal slope conductance value of 94 pS at +100 mV applied to the *cis* side of the bilayer. Under these conditions, a different single-channel activity of lesser conductance became apparent above the γ_{MS} current at positive membrane potentials. Also in 10 mM Ca^{2+} solutions, Mg^{2+} permeates through the main channel when added to the *cis* side with a $P_{Ca}/P_{Mg} = 2.9$, while it blocks when added to the *trans* side. In 50 mM Ca^{2+} solutions, the γ_{MS} open probability has values of 1.0 at voltages more positive than −40 mV and decreases at more negatives potentials, following a Boltzmann function with an $E_{0.5} = -72$ mV and an apparent gating charge value of 3.9. These results describe a novel Ca^{2+}-selective channel, and suggest that the main channel works as a single multipore assembly.

INTRODUCTION

Ion fluxes across the sea urchin sperm plasma membrane play an important role in the physiology of this cell. It is known that when sperm reach the outermost investment of the egg, the "egg jelly," they undergo the acrosome reaction (AR). The AR

Address reprint requests to Dr. A. Darszon, Department de Bioquímica, Centro de Investigación y de Estudios Avanzados del Instituto Politécnico Nacional Apartado Postal 14-740, 07000 México D.F., México

J. GEN. PHYSIOL. © The Rockefeller University Press · 0022-1295/90/02/0273/24 $2.00
Volume 95 February 1990 273–296

involves several morphophysiological changes; among the more important are: Na^+ and Ca^{2+} influxes and K^+ and H^+ effluxes (Schackmann et al., 1978; Schackmann and Shapiro, 1981; Darszon et al., 1988), increases in both cGMP and cAMP intracellular concentrations (Garbers and Hardman, 1975; Kopf and Garbers, 1980), intracellular accumulation of inositol 1,4,5-trisphosphate (Domino and Garbers, 1988) and the formation of the acrosome tubule. The Na^+ influx and the H^+ efflux are apparently linked stoichiometrically (Schackmann and Shapiro, 1981), and there are reports showing the presence of an electroneutral, voltage-dependent Na^+/H^+ exchanger in the sperm flagellum (Lee, 1984, 1985). Concerning the Ca^{2+} and K^+ movements across the sperm plasma membrane, there is pharmacological evidence indicating that ionic channels participate in the triggering mechanism of the egg jelly–induced AR (Schackmann et al., 1978; Kazazoglou et al., 1985; Darszon et al., 1987).

There is only one report demonstrating the existence of ionic channels in the sea urchin sperm in vivo (Guerrero et al., 1987). However, the high difficulty of these experiments due to the small size of the sea urchin sperm head (~2 μm in diameter) has prevented a proper study of channel selectivity and kinetics. As an alternative way to study the ionic channels present in the sea urchin sperm plasma membrane, a reconstitution approach is being used. Previously, the existence of K^+ channels in the sperm plasma membrane was detected, by incorporating isolated membranes into a bilayer made at the tip of a patch-clamp microelectrode (Liévano et al., 1986).

This report describes the cationic channels found fusing sea urchin sperm plasma membrane vesicles with preformed lipid bilayers made in divalent cation solutions. The channels detected are strongly voltage dependent, and show a very complex current pattern at negative holding potentials. They are able to conduct Ca^{2+}, Sr^{2+}, and Ba^{2+}, and display a slightly higher selectivity toward divalent over monovalent cations. Interestingly, Mg^{2+} ions can permeate the channels when added to the *cis* chamber, but block when added to *trans*. The inorganic blockers Cd^{2+} and Co^{2+} ions at millimolar concentrations block both the channels described here and the egg jelly–induced acrosome reaction in whole sperm. A preliminary report of part of this work has appeared in abstract form (Liévano et al., 1988).

MATERIALS AND METHODS

Sea urchins (*Strongylocentrotus purpuratus*) were obtained from Pacific Bio-Marine Laboratories Inc., (Venice, CA) and kept in a temperature-controlled instant ocean aquarium. Spawning was induced by intracoelomic injection of 0.5 M KCl. Sea urchin sperm plasma membranes used were preferentially derived from the flagella, and were isolated according to the method of Cross (1983), with the previously described modifications (Darszon et al., 1984). The membrane vesicles were preloaded with 0.6 M sucrose by sonication (2 min) with a bath sonifier (model B12, Branson Cleaning Equipment Co., Shelton, CT) to give them an appropriate osmotic gradient for the fusion with the bilayer (Cohen et al., 1980), and were stored at −70°C until use. The membrane preparations were never older than 6 mo. The determination of the percentage of sperm acrosome reaction was done by using phase contrast microscopy, and the $^{45}Ca^{2+}$ uptake measurements were performed as described previously (García-Soto and Darszon, 1985).

Planar Lipid Bilayers and Solutions

Black lipid bilayers were made by the Müller-Rudin method (Müller and Rudin, 1969), and the plasma membrane vesicles were incorporated into them using the fusion strategy (Miller and Racker, 1976). The bilayers were formed both with a mixture of phosphatidylethanolamine (PE) and phosphatidylserine (PS) from bovine brain or with synthetic diphytanoylphosphatidylcholine (DiPhyPC) dispersed in *n*-decane at a concentration of 20 mg/ml. (all from Avanti Polar Lipids, Inc., Birmingham, AL). The bilayer chamber had two 400-μl compartments, and the bilayers were painted on a hole made by an electrical spark (Hartshorne et al., 1986) on a plastic partition (Saran Wrap, Dow Chemical Co., Indianapolis, IA). The hole diameter was between 200 and 280 μm, and was pretreated with the same lipid dispersion used for bilayer formation as in (Hartshorne et al., 1986) before bilayer formation. The lipid solution was applied to the hole with a fire-rounded glass capillary tube. Bilaver formation was followed by measuring the capacitative current in response to a square voltage pulse. Only those bilayers with a capacitance higher than 200 pF were used. In all the experiments, the *cis* chamber was the side of addition of the membrane fraction, and also where the voltages were applied. *Trans* chamber was at virtual ground.

Once the bilayer was formed, it was left undisturbed for ~10 min, and after this time pulses of ±100 mV were applied for 30 s to check that the bilayer did not show any single-channel–like activity. Thereafter, the membrane potential was clamped at +50 mV and the membrane vesicles were added to the *cis* side of the chamber, at a protein concentration between 5 and 25 μg/ml. After some time, typically between 1 and 30 min, the fusion of the membrane vesicles to the lipid bilayer was observed, with single-channel activity apparent.

In the experiments with a $Ba(HEPES)_2$ gradient across, the *cis* chamber was filled with a 200 mM solution, pH 8.0, and the *trans* chamber with a 40 mM solution, pH 8.0. After this, the bilayer was painted as already described.

For the experiments in which a $CaCl_2$ gradient was used, the bilayer was initially formed in symmetrical 50 mM $CaCl_2$, 10 mM HEPES-TMA (tetramethyl ammonium), pH 8.0 solutions. To achieve the desired concentration, the required amount of concentrated stock solution was added to the *cis* chamber.

In the Mg^{2+} experiments, the bilayers were formed in a solution containing 10 mM $CaCl_2$, 5 mM Tris-Cl, pH 8.0. Once a channel was incorporated the *I-V* control records were taken, and afterwards an aliquot of concentrated $MgCl_2$ solution, enough to raise the Mg^{2+} concentration to 50 mM, was added to the *cis* or *trans* side of the chamber; then stirring with a magnetic bar was applied for 1 min. Thereafter, the bilayer was left undisturbed for 4 min.

In the biionic experiments, the bilayer was formed in symmetrical 100 mM monovalent cation, 10 mM HEPES-TMA, pH 8.0, and then the *cis* chamber was perfused with at least 10 times its volume with a solution of the test 50 mM divalent cation, 10 mM HEPES-TMA, pH 8.0. The solution change was performed by injecting the test solution with a peristaltic pump. A glass capillary tube connected to a vacuum pump at the level of the solution meniscus was used to avoid sudden changes in the hydrostatic pressure during the solution change. The bilayer was left undisturbed for ~5 min and then the membrane vesicles were added to the *cis* side of the chamber. The Fatt-Ginsborg derivation of the Goldmann-Hodgkin-Katz equation was used for the calculation of the ratio of permeability coefficients between divalent over monovalent cations:

$$\frac{P_{C^{2+}}}{P_{C^+}} = \frac{\gamma_{c^{2+}}[C^{2+}]cis}{4\gamma_{c^+}[C^+]trans}\left[\frac{1 + e^{-(FE_r/RT)}}{e^{(FE_r/RT)}}\right] \quad (1)$$

in which γ_{c^+} and $\gamma_{c^{2+}}$ correspond to the monovalent and divalent cation activity coefficients, respectively, C^+ and C^{2+} indicate monovalent and divalent cation, respectively, $[C^+]trans$ and

$[C^{2+}]cis$ are their concentrations in *cis* and *trans*, E_r is the measured reversal potential value, and the expression (FE_r/RT) has its usual meaning.

For divalent cations, the following equation (kindly derived by Froylán Gómez-Lagunas) was used.

$$\frac{P_{C_2^{2+}}}{P_{C_1^{2+}}} = \frac{\gamma_{c_1^{2+}}[C_1^{2+}]trans - \gamma_{c_1^{2+}}[C_1^{2+}]cis\, e^{(2FE_r/RT)}}{\gamma_{c_2^{2+}}[C_2^{2+}]cis\, e^{(2FE_r/RT)} - \gamma_{c_2^{2+}}[C_2^{2+}]trans} \quad (2)$$

To obtain the single divalent cation activity coefficients, the Guggenheim convention was applied: $\gamma_{c^{2+}} = (\gamma_{ccl_2})^2$, and for the monovalent cations it was assumed that the ion activity was the mean activity coefficient for the chloride salt. The solution mean activity coefficients were taken from Harned and Owen (1958).

For the experiments with blockers, the records were taken before (control) and after the blocker (Cd^{2+}, Co^{2+}, or La^{3+}) was added to the indicated final molarity from high concentration stock solutions. The bilayer was left undisturbed for 5 min before taking the current records.

Data Acquisition and Analysis

The current to voltage transducer was based on an OPA111A operational amplifier (kindly provided by Dr. R. French, University of Calgary, Calgary, Canada) with a 1GΩ resistor in the feedback loop. The transducer time constant was ~150 μs. The electrodes were made from a chlorided silver wire immersed in agar bridges (4% agar in 1 M KCl).

Channel currents were recorded on a video-cassette recorder (SL 2700; Sony, Tokyo, Japan) and a modified digital-audio processor data acquisition and storage system; Unitrade Inc., Philadelphia, PA) as described (Bezanilla, 1985). The channel current records, unless otherwise stated, were usually filtered at 800 Hz (−3 db point) with an eight-pole Bessel filter (744PL-3 and 744PL-4 modules connected in series; Frequency Devices, Inc., Haverhill, MA), and were digitized off-line at a speed of 2 kHz with a 12-bit analog to digital converter (Labmaster; Scientific Solutions, Inc., Solon, OH) connected to an AT computer.

To study the channel conductance states at negative potentials, the single-channel current step sizes were initially measured by hand. To more efficiently resolve the open probability of the several states of the channel at negative potentials, a computer program was designed to measure the time the channel spent in each one of the current levels present. The program builds the corresponding current vs. time histograms. The several peaks appearing, each one roughly following a normal distribution, were selected manually. The area under them was calculated according to a normal distribution equation by taking the corresponding current peak value, and the record noise standard deviation. The open probability of each one of the current states of the channel was estimated as the time the channel spent in this state, divided by the total record time. The program will be described in detail elsewhere.

The data correspond to 82 recorded bilayers, which is equivalent to 38 h of current records. Channels were incorporated with the same orientation, as judged by the voltage dependence, and the current pattern in >95% of the experiments.

RESULTS

Incorporation of the Channels into Lipid Bilayers

The addition of the sperm membrane fraction to a lipid bilayer leads to the incorporation of ion channels. Fig. 1 *A* shows typical current records of the ion channel activity detected after fusing the sperm plasma membrane fraction with a DiPhyPC bilayer formed in symmetrical solution of 50 mM $CaCl_2$, 10 mM HEPES-TMA, pH

8.0. The complex voltage-dependent behavior of the channel was evident in the records taken at negative potentials in Fig. 1 *A*. At E_m values between +100 and −25 mV there was only a main conducting level of current, but at potentials equal or more negative than E_m = −50 mV, the channel activity started at the main level of current and rapidly decayed, in a nonstationary way, to several other current levels of lesser conductance. At more negative E_m values the channel spent less time in the main conducting state. In the −75 and −100 mV records, it is difficult to notice the short time the channel spent in the main conducting state, because (due to the large

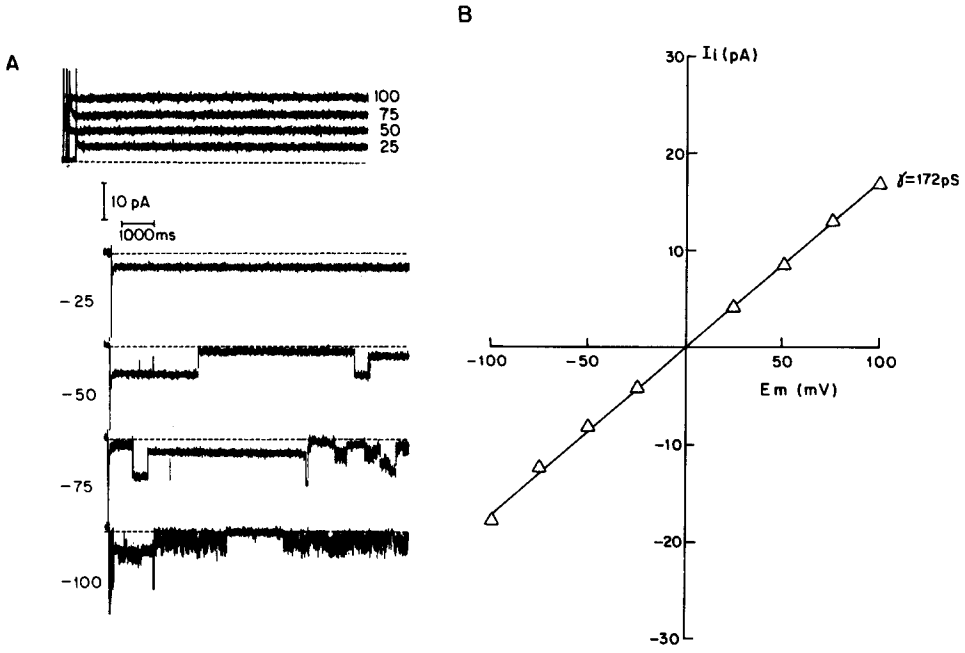

FIGURE 1. (*A*) Current records of the channel incorporated into a DiPhyPC lipid bilayer at different holding potentials in symmetrical $CaCl_2$ 50 mM, 10 mM HEPES-TMA, pH 8.0 solutions. The upper part shows current records obtained at the positive membrane potentials in mV indicated on the right. The lower part shows the current records obtained at negative E_m, whose value is indicated by the number at the left side of each record. The dashed line indicates the zero-current level. The currents were filtered at 800 Hz and digitized at 2 kHz. (*B*) *I-V* curve from the main-state conductance obtained from six bilayers similar to that depicted in *A*. The standard deviation was <5% in all the experimental points, and the slope was obtained by linear regression giving a γ_{MS} of 172 pS.

time scale used) its corresponding current is almost buried in the capacitative transient at the beginning of the voltage pulse. The *I-V* curve of the channel's main-state (γ_{MS}) is shown in Fig. 1 *B*. It was ohmic between −100 and +100 mV and had a single-channel conductance value of 172 pS.

There were different current step sizes associated with the channel activity at negative potentials. Fig. 2 *A* illustrates four consecutive traces of a record taken at E_m = −100 mV for a longer time; the presence of single-channel current steps of different sizes are evident. Fig. 2 *B* shows that the *I-V* curves of the observed current

step sizes from experiments similar to those just described were all linear. The conductances of the current steps were smaller than γ_{MS}, and since they do not occur at positive potentials, only the currents obtained at negative holding potentials are shown. The γ_{MS} should not be confused with the different conductances of the current steps. Transitions from the γ_{MS} to zero were never observed, which explains the difference in the conductance values between γ_{MS} and the larger one shown in Figs. 2 *B*, 4, *A* and *C*, and 5, *A* and *C*.

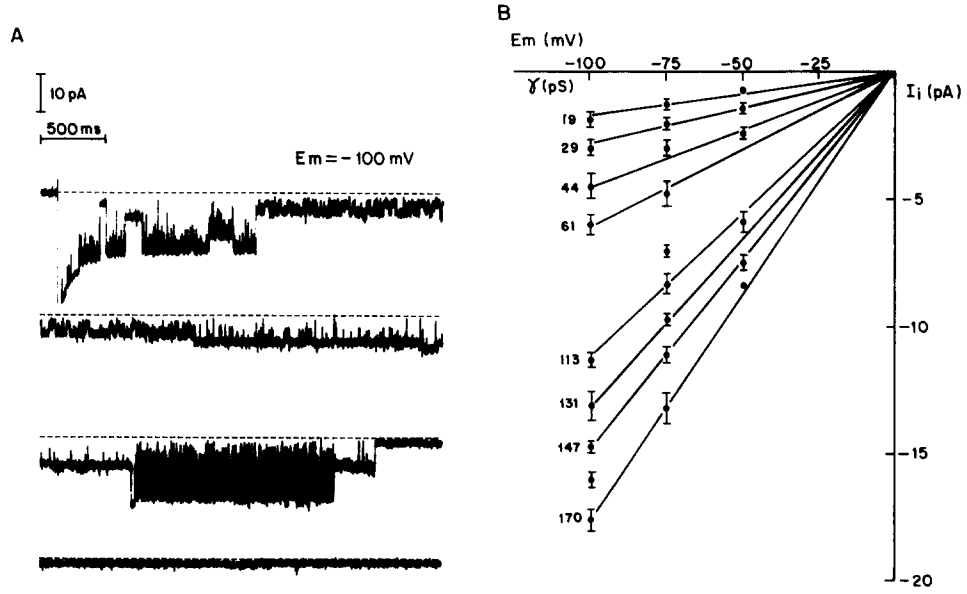

FIGURE 2. (*A*) Consecutive records obtained from a channel incorporated into a DiPhyPC bilayer in 50 mM $CaCl_2$, 10 mM HEPES-TMA, pH 8.0 at $E_m = -100$ mV. Record conditioning was as in Fig. 1 *A*. (*B*) *I-V* curves obtained from the observed current steps in bilayers in which there was only one channel incorporated, under the same experimental conditions as in Fig. 1 *A*. The data points were obtained from five bilayers, and each point represents at least five data points. The number at the left side of each curve represents the conductance in picosiemens.

Selectivity of the Incorporated Channels

The selectivity of the channel was studied with a salt gradient across planar bilayers made of PE/PS (1:1), using HEPES as the anion to avoid interference of an anionic channel previously reported (Liévano et al., 1986). Fig. 3 *A* shows typical current records obtained from the fusion of one channel into a lipid bilayer exposed to a gradient of $Ba(HEPES)_2$: 200 mM *cis* and 40 mM *trans*, pH 8.0. In the upper part the currents obtained at the indicated positive membrane potentials are displayed. The dashed line at the bottom of the positive records indicates the zero-current level. The lower part of Fig. 3 *A* shows current records obtained at negative E_m. The zero-current level is shown in each record in the upper part. A positive current was evident at $E_m = 0$ mV, corresponding to γ_{MS}, and it reversed at $E_r = -14 \pm 3$ mV ($n = 5$; $E_{Ba^{2+}} = -20$ mV, without correcting for the Ba^{2+} activity coefficients). Fig. 3 *B* shows that the *I-V* curve obtained from similar experiments was linear even

though asymmetrical solutions were used to form the bilayer. The value of γ_{MS} was 270 pS. The linearity of the curve indicates that the channel γ_{MS} is already saturated at 40 mM of permeant cation in *trans*. In agreement with this, the experiments done in 50 mM $BaCl_2$ solutions (Fig. 5 *A*, below) gave a similar γ_{MS} value (266 pS) and a linear *I-V* curve.

In another set of experiments in which the channel was inserted into neutral DiPhyPC bilayers with a $CaCl_2$ gradient across (300 mM *cis*, 50 mM *trans*, HEPES-TMA 10 mM, pH 8.0), a positive current also corresponding to the γ_{MS} became evident at zero applied potential. Its reversal potential was $E_r = -16.8 \pm 1.5$ mV

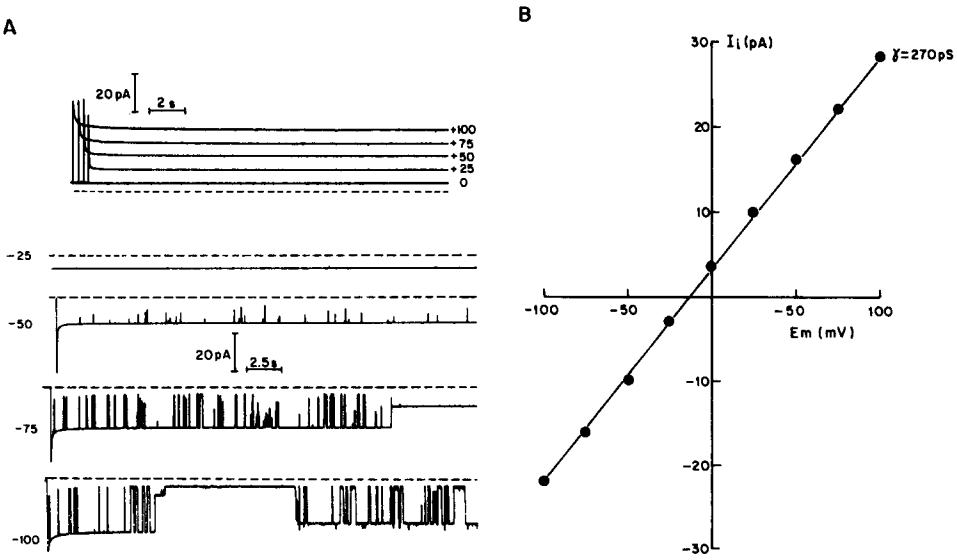

FIGURE 3. (*A*) Current traces from a channel incorporated into a PE/PS lipid bilayer in a $Ba(HEPES)_2$, pH 8.0 solution (200 mM *cis*, 40 mM *trans*). The upper traces represent the records taken at positive E_m, whose value in millivolts is indicated on the right-hand side. The dashed line at the bottom indicates the zero-current level. The lower traces were taken at negative E_m (number on the left-hand side). The upper dashed line in each record indicates the zero-current level. Current records were filtered at 100 Hz, and digitized at 500 Hz. The rise of the capacitative current resulting from the voltage pulse is shown in all records with the exception of the one taken at −25 mV. (*B*) *I-V* relation of the main-state conductance obtained from five experiments similar to that shown in *A*. E_r was -14.1 ± 0.7 mV, and the conductance value was 270 pS.

($n = 3$). In these experiments, $E_{Ca^{2+}} = -17.3$ mV, obtained by using the Ca^{2+} ion activity in the Nernst equation. The above results indicate that the channel incorporated in the bilayers was cationic and imply that it was able to exclude anions, in spite of its high single-channel conductance in divalent cation solutions.

Sr^{2+} *and* Ba^{2+} *as Charge Carriers*

The behavior of the channel with divalent cations other than calcium was studied in neutral DiPhyPC bilayers made in both $SrCl_2$ and in $BaCl_2$ solutions. Fig. 4 *A* shows

the *I-V* curves of the γ_{MS} of the channel in 50 mM $SrCl_2$, 10 mM HEPES-TMA, pH 8.0, whereas Fig. 4 *B* shows typical current records at different membrane potentials. In this solution, the γ_{MS} was 220 pS, and the channel displayed a complex pattern of current fluctuations with Sr^{2+} as the charge carrier. Fig. 4 *C* shows the *I-V* relations of the measured current step sizes. Eight different conductances were apparent. In 50 mM $BaCl_2$, the γ_{MS} was 266 pS (see Fig. 5 *A*). The pattern of current fluctuations (Fig. 5 *B*), as well as the measured current steps (Fig. 5 *C*) were similar to those found both in Ca^{2+} and in Sr^{2+} solutions. The above results indicate that the channel incorporated in planar bilayers was able to conduct Ba^{2+}, Sr^{2+}, and Ca^{2+}, and the γ_{MS} values follow the sequence $Ba^{2+} > Sr^{2+} > Ca^{2+}$. This divalent cation conductance sequence occurs in calcium channels from other biological preparations (Hagiwara and Byerly, 1981; Tsien et al., 1987).

Voltage Dependence of the Main-State Conductance

To analyze the channel's complex nonstationary current patterns at negative potentials in another way, a program was designed to build the histograms of the current levels and the time the channel spent at each level (see the Methods section). The channel decays randomly to the smaller subconducting states shortly after the rise of the pulse at negative potentials indicating that it undergoes some sort of "inactivation." If left for an adequate amount of time at an inactivating voltage, the channel closes even to the zero-current level; it was difficult to observe transitions from the lesser conducting levels to the γ_{MS}. Thus, instead of DC potentials, five 10-s pulses were taken to construct statistically significant histograms of the γ_{MS} open probability at each E_m. Fig. 6 shows typical histograms obtained from the channel at different E_m values in 50 mM Ba^{2+}, 10 mM HEPES-TMA, pH 8.0. Since the histograms were constructed by alternating positive and negative pulses of the same magnitude, both positive and negative currents (shown as filled peaks) are displayed in the histograms. This was done to illustrate graphically the voltage dependence of the channel. The conductance values in picosiemens corresponding to the current peaks are indicated by the numbers at the top. Fig. 7 shows the open probability from the γ_{MS} as a function of E_m obtained from the current vs. time. The curve follows a Boltzmann function, with an $E_{0.5} = -72$ mV. The best fit on data gave an apparent gating charge value of 3.9.

Current Levels Appearing at Negative Potentials

Current histograms (not shown) were also obtained for experiments with the other divalent cations tested. Fig. 8 illustrates the channel conductances corresponding to the different current levels observed in experiments made in 50 mM Ca^{2+}, Sr^{2+}, and Ba^{2+} solutions, vs. the sublevel number. The sublevel numbers were assigned in a decreasing order according to their γ values. The resulting conductances appeared to follow, in general, the size sequence of the γ_{MS} in each one of the divalent cations tested.

Vectorial Mg^{2+} Effect on the Channel Behavior

Mg^{2+} ions are present at a high concentration in seawater, ~60 mM, while Ca^{2+} is 10 mM. To evaluate the effect of Mg^{2+} on the channel, control records were made

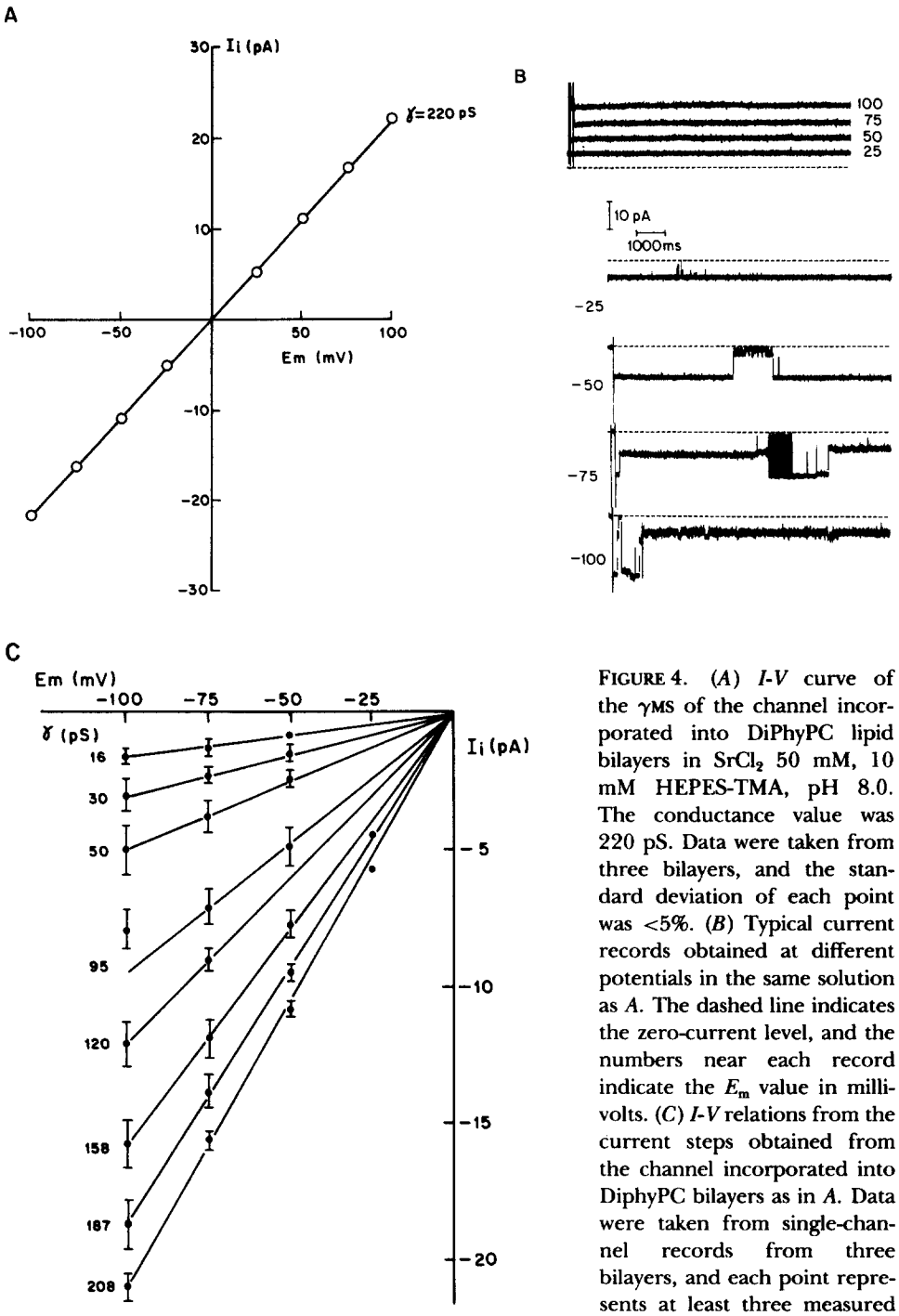

FIGURE 4. (*A*) *I-V* curve of the γ_{MS} of the channel incorporated into DiPhyPC lipid bilayers in $SrCl_2$ 50 mM, 10 mM HEPES-TMA, pH 8.0. The conductance value was 220 pS. Data were taken from three bilayers, and the standard deviation of each point was <5%. (*B*) Typical current records obtained at different potentials in the same solution as *A*. The dashed line indicates the zero-current level, and the numbers near each record indicate the E_m value in millivolts. (*C*) *I-V* relations from the current steps obtained from the channel incorporated into DiphyPC bilayers as in *A*. Data were taken from single-channel records from three bilayers, and each point represents at least three measured current steps in each one of the bilayers.

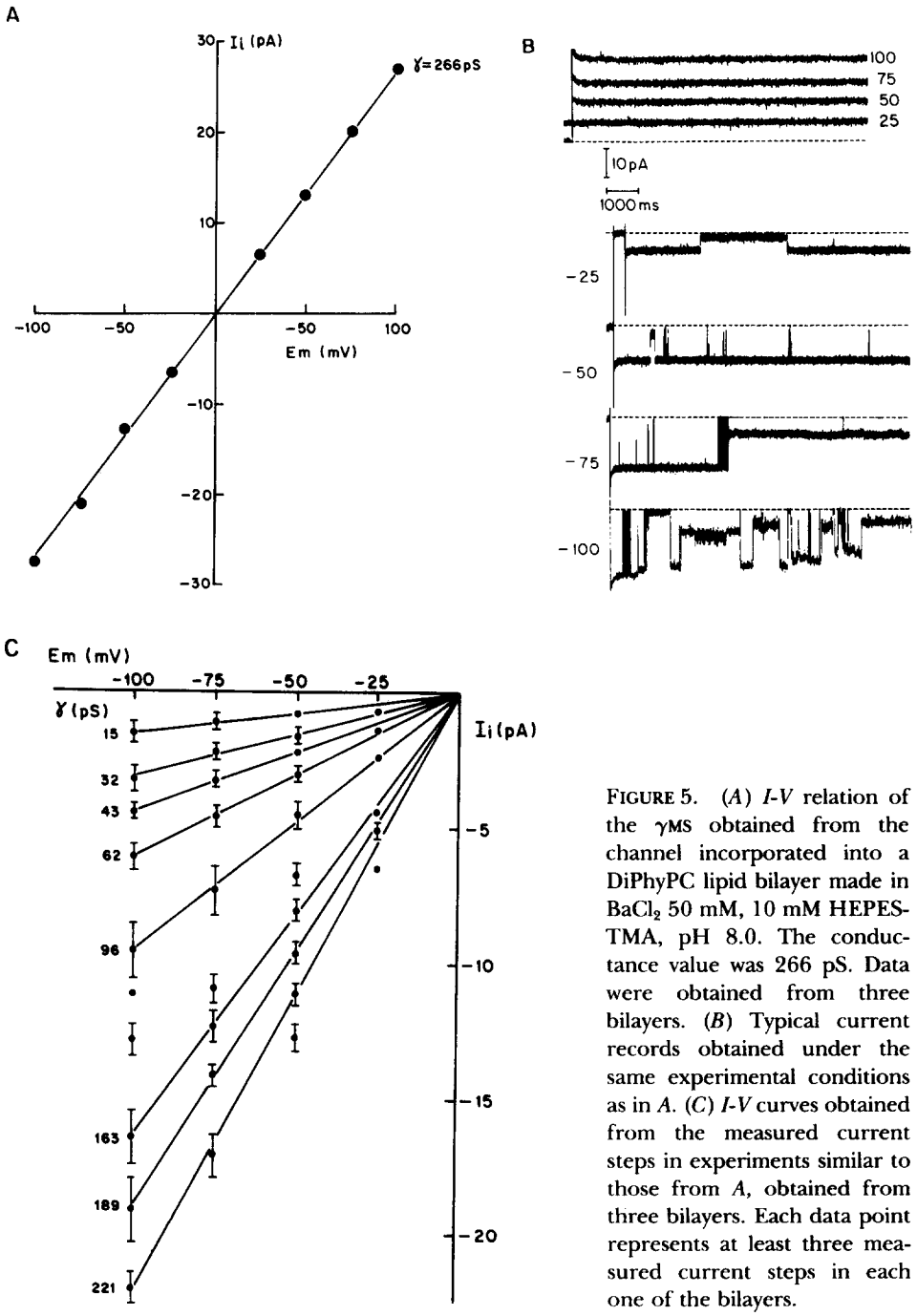

FIGURE 5. (*A*) *I-V* relation of the γMS obtained from the channel incorporated into a DiPhyPC lipid bilayer made in $BaCl_2$ 50 mM, 10 mM HEPES-TMA, pH 8.0. The conductance value was 266 pS. Data were obtained from three bilayers. (*B*) Typical current records obtained under the same experimental conditions as in *A*. (*C*) *I-V* curves obtained from the measured current steps in experiments similar to those from *A*, obtained from three bilayers. Each data point represents at least three measured current steps in each one of the bilayers.

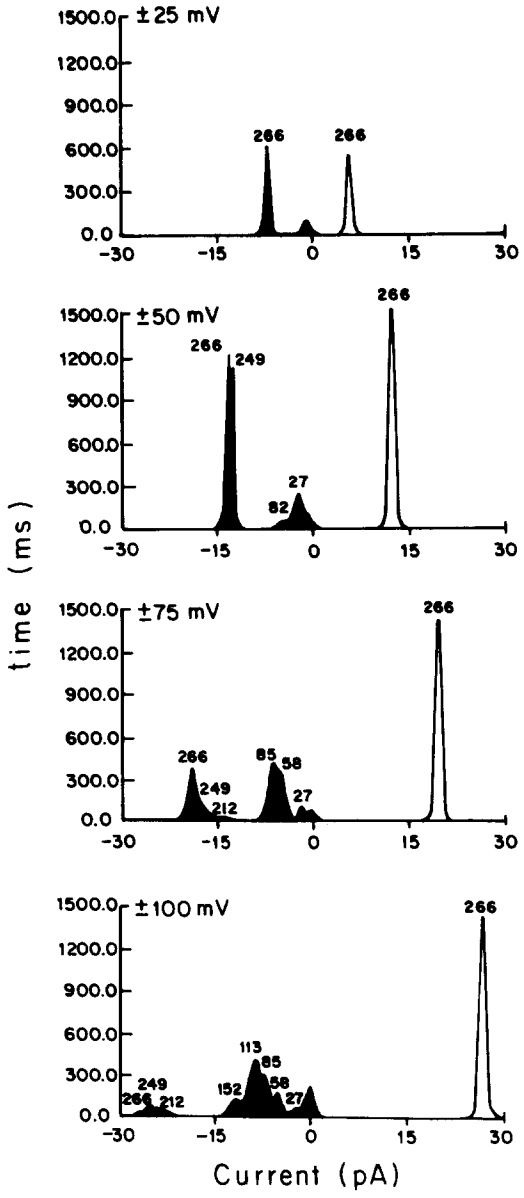

FIGURE 6. Current level histograms of a channel incorporated into a DiPhyPC bilayer in 50 mM $BaCl_2$, 10 mM HEPES-TMA, pH 8.0. The histograms were made by taking 90-s current records at alternating positive and negative (filled current peaks) voltage pulses of the same magnitude, lasting 5 s. The upper histogram was constructed taking only 30 s. The number over each one of the current peaks corresponds to its conductance value.

in symmetrical 10 mM $CaCl_2$, 5 mM Tris-Cl, pH 8.0. The *I-V* curve of the γMS (Fig. 9 *A*, *open circles*) rectified under these ionic conditions, having a maximal value of 94 pS at an E_m of +100 mV. In these experiments, a different voltage-dependent conductance over the γMS at positive potentials became evident (~48 pS); this was not observed at higher Ca^{2+} concentrations (50–100 mM; see left side of Fig. 9 *B*). The addition of 50 mM $MgCl_2$ to the *cis* side of the chamber gave a positive current at zero holding potential, as shown in Fig. 9 *A* (*closed circles*), indicating that Mg^{2+} was

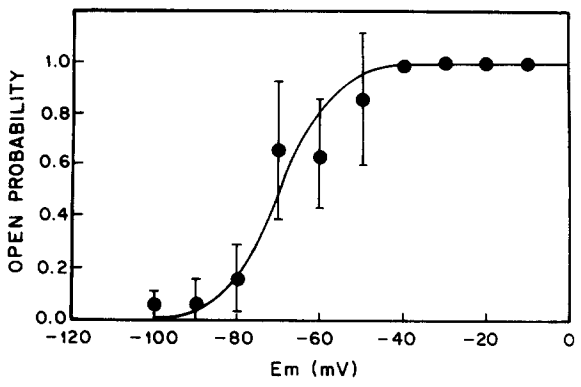

FIGURE 7. γ_{MS} open probability as a function of the applied E_m. Data were obtained from the channel current histograms of five DiPhyPC bilayers made in 50 mM $CaCl_2$, 5 mM Tris-Cl, pH 8.0. The histograms of each bilayer were constructed by taking five pulses, lasting 10 s at the indicated E_m values. Each data point represents the mean ± SD, and the solid line was drawn according to the equation: $P_o = 1/\{1 + e^{[qF(E_{0.5}-E_m)/RT]}\}$, with an $E_{0.5}$ of −72 mV and an apparent gating charge (q) of 3.9.

able to pass across the channel. The reversal potential of this current was −35 mV, giving a P_{Ca}/P_{Mg} ratio of 2.8, as calculated with the Goldmann-Hodgkin-Katz equation for divalent cations. However, when Mg^{2+} was added to the *trans* side, a voltage-independent blocking effect was observed (see Fig. 9 *B*, right side). Mg^{2+} in the *trans* side did not appear to block the channel by occlusion, since the effect occurred at positive *cis*-applied potentials, against the Mg^{2+} electrochemical potential. The Mg^{2+} blocking mechanism remains to be studied in more detail, but it could be that there is a binding site to this ion that affects the behavior of the channel.

Effect of Inorganic Ca^{2+} Channel Blockers

Since the channel allows divalent cations to permeate, Cd^{2+}, Co^{2+}, and La^{3+}, which are known blockers of calcium channels in several preparations (Hagiwara and

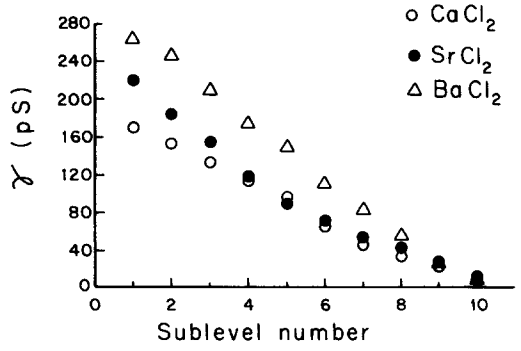

FIGURE 8. Conductance values from the current sublevels appearing at negative membrane potentials. Experiments were made in 50 mM $CaCl_2$ (*open circles*), $SrCl_2$ (*closed circles*), and $BaCl_2$ (*open triangles*), 10 mM HEPES-TMA, pH 8.0. The channels were incorporated into neutral DiPhyPC lipid bilayers. Data were obtained from the current histograms from three bilayers for Ba^{2+} and Sr^{2+} and from five bilayers for Ca^{2+}. In all cases, the standard deviation was <5%. The sublevel numbers were assigned in a decreasing order according to their γ values in picosiemens.

Byerly, 1981), were tested. Fig. 10 illustrates the effect of adding increasing concentrations of $CdCl_2$ to both chambers on the γMS of the channel incorporated in PE/PS bilayers under symmetrical conditions, in a solution of 40 mM $Ba(HEPES)_2$, pH 8.0. The inset shows the normalized blocking curve as a function of $CdCl_2$ concentration. The $K_{0.5}$ value obtained was 20 mM. Table I shows the effect of $CdCl_2$ on

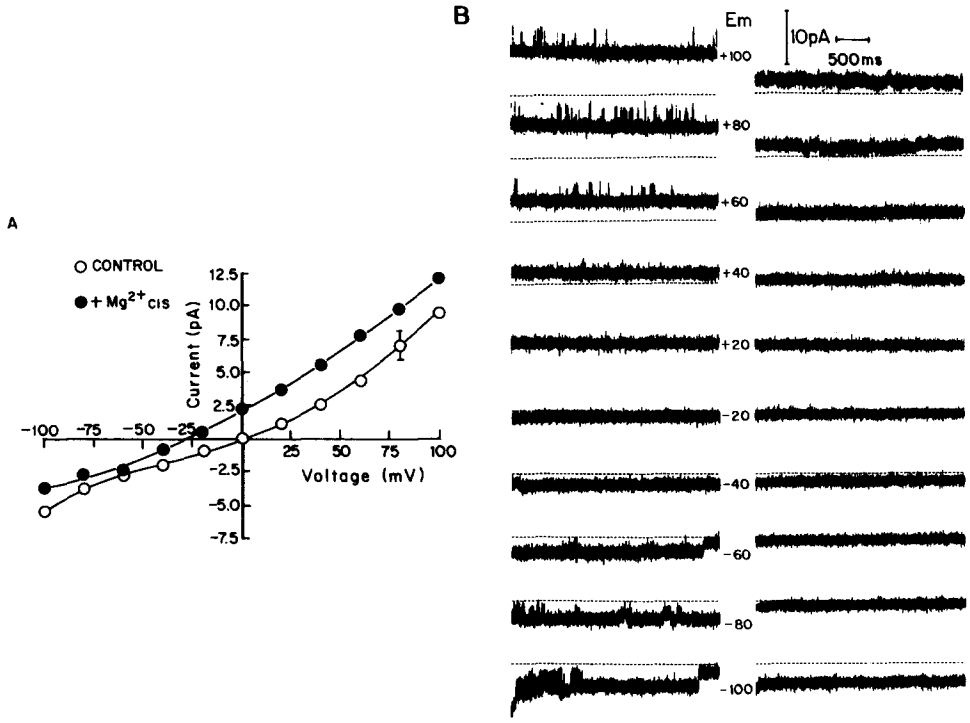

FIGURE 9. (*A*) Effect of $MgCl_2$ on the Ca^{2+} current across the channel. The channel was incorporated into DiPhyPC bilayers made in 10 mM $CaCl_2$, 5 mM Tris-Cl, pH 8.0. Open circles correspond to the control experiment, and the closed ones to the currents obtained after the addition of 50 mM $MgCl_2$ to the *cis* side of the bilayer. The measured E_r value was -35.2 ± 2.8 ($n = 5$). The lines between the experimental points were obtained with a polynomial regression, and do not have any theoretical meaning. Data were taken from five bilayers, and the SD was <5%. (*B*) Current records from experiments similar to those described in *A*. The records on the left side correspond to the control conditions, and the right-hand ones were obtained after adding 50 mM symmetrical $MgCl_2$. The numbers between the left and right records indicate the membrane potential. The records were filtered at 800 Hz, and digitized at 2 kHz. Each record corresponds to 3.2 s.

the step-size conductances measured at negative holding potentials. All the conductances were apparently reduced in a similar fashion. Interestingly Cd^{2+} also blocked the egg jelly–induced acrosome reaction and its associated $^{45}Ca^{2+}$ uptake at similar concentrations (see Table II).

Fig. 11 illustrates the blocking effect of Co^{2+}. The left side shows control current records taken at positive potentials from a DiPhyPC bilayer made in 50 mM $SrCl_2$,

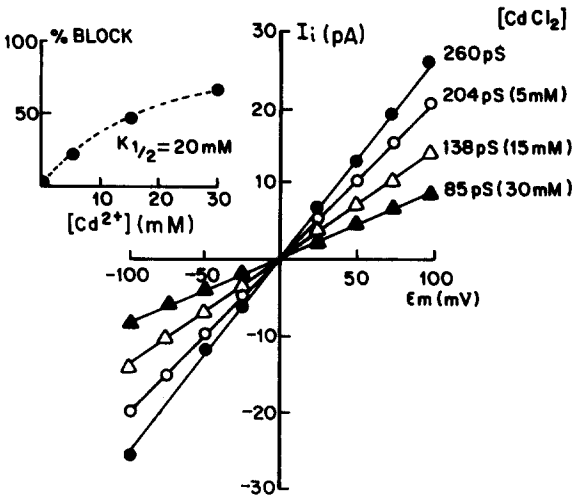

FIGURE 10. Blocking effect of Cd^{2+} on γMS. *I-V* curves from channels incorporated into PE/PS 1:1 bilayers (n = 5) made in 40 mM $Ba(HEPES)_2$, pH 8.0 at different $CdCl_2$ concentrations. The number on the right side indicates the γMS, and the number enclosed in brackets indicates the [$CdCl_2$] symmetrical concentration. The inset shows the normalized blocking curve, having a $K_{0.5}$ of 20 mM.

10 mM HEPES-TMA, pH 8.0 with two channels incorporated. The current records on the right side show the effect of 20 mM $CoCl_2$ added to the *cis* chamber. It is evident that both the open probability and the current amplitude of the channels were affected by the blocker. The blocking behavior of Co^{2+} will be characterized in detail in future studies. In addition, the channel was completely blocked by 5 mM of $LaCl_3$ in the *cis* side of the chamber (n = 3, data not shown).

Divalent/Monovalent Cation Permeability Coefficient Ratios

To determine the channel selectivity toward monovalent cations, biionic experiments were done, in which the bilayer was formed in symmetrical 100 mM monova-

TABLE I

Cd^{2+} Block of the Current Transitions

Control	$CdCl_2$ symmetrical concentration		
	+5 mM	+15 mM	+25 mM
262	238 ± 5	183 ± 9	
232 ± 1	201 ± 7	148 ± 10	63
202 ± 9	174 ± 3	123 ± 10	55
179 ± 9	157 ± 3		
142 ± 5	130 ± 5	100 ± 3	44
106 ± 7	101 ± 8	79 ± 3	
79	75 ± 3	60 ± 7	20
	60 ± 1	35 ± 2	
56 ± 2			
46	42 ± 2		
32 ± 1	24 ± 3	23 ± 1	
21	15	13	

Experiments were conducted as in Fig. 10. Data were taken from five bilayers, and each point represents the mean of the measurements of many step sizes in each bilayer. Data without standard deviations correspond to several step currents of similar conductance measured in at least two bilayers.

TABLE II

Cd^{2+} Block of Egg Jelly–induced Acrosome Reaction and $^{45}Ca^{2+}$ Uptake in Whole Sperm

[$CdCl_2$]	Percent $^{45}Ca^{2+}$ uptake	Percent acrosome reaction
mM		
0.0	100 ± 0	100 ± 0
0.01	74 ± 2	100 ± 0
0.1	69 ± 1	96 ± 4
1.0	44 ± 20	66 ± 9
10.0	29 ± 9	19 ± 7
50.0	28 ± 10	7 ± 1

The results were obtained from five experiments. For the $^{45}Ca^{2+}$ uptake, 100% corresponded to 26 nmol of $^{45}Ca^{2+}$ taken by 10^8 cells, corrected by the basal sperm $^{45}Ca^{2+}$ uptake. The egg jelly–induced acrosome reaction was scored as described in the Methods section.

lent cation (Na^+ or K^+), HEPES-TMA pH 8.0. After 10 min the solution in the *cis* chamber was exchanged for 50 mM divalent cation (Ca^{2+}, Sr^{2+}, or Ba^{2+}), HEPES-TMA, pH 8.0 as already described, and then the membrane vesicles were added. In all the conditions, a steady positive current across the channel at zero potential was observed when fusion occurred, corresponding to the γMS in response to the biionic gradient. The zero-current potentials obtained with the experiments done with a divalent cation in the *cis* side and a monovalent one in the *trans* side are shown in the

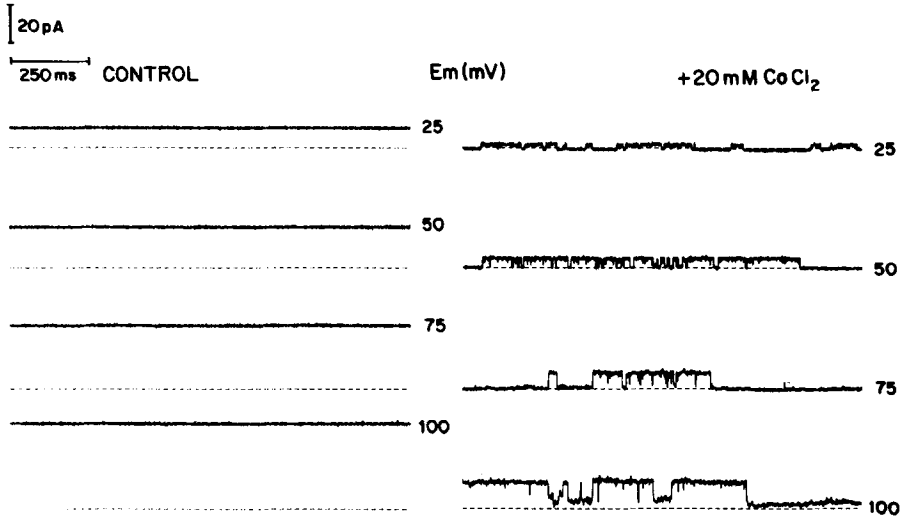

FIGURE 11. Blocking effect of Co^{2+} on γMS. The records on the left side show the main-state current from two channels incorporated into a DiPhyPC bilayer made in 50 mM $SrCl_2$, 10 mM HEPES-TMA, pH 8.0. The right side displays the records obtained after adding 20 mM $CoCl_2$ to *cis* chamber. The right-hand number in each record indicates the E_m, and each record lasts 1.2 s.

upper part of Table III. A comparison of the ratios of the permeability coefficients for divalent vs. monovalent cation calculated with the Goldmann-Hodgkin-Katz equation appear in the lower section of table III. Clearly the channel is poorly selective towards divalent over monovalent cations.

TABLE III

E_r Values from Biionic Experiments

Cis	*Trans*	
	Na^+	K^+
	mV	
Ca^{2+}	−14.0 ± 0.6 (4)	−5.7 ± 0.5 (3)
Ba^{2+}	−13.1 ± 0.7 (3)	−8.1 ± 1.0 (3)
Sr^{2+}	−14.9 (1)	—

Relative permeability values

P_{Ca}/P_{Na} = 5.9	P_{Ca}/P_K = 3.4
P_{Ba}/P_{Na} = 5.5	P_{Ba}/P_K = 3.9
P_{Ca}/P_{Mg} = 2.8*	

γ_{MS} reversal potential obtained from biionic experiments and permeability coefficient ratios. The channel was incorporated into DiPhyPC bilayers bathed in 50 mM divalent cation chloride in *cis*, and 100 mM monovalent cation chloride in *trans*, 10 mM HEPES-TMA, pH 8.0 in all tested combinations. The upper part shows the reversal potential, which was obtained by measuring the membrane potential required to cancel the current across the channel. The numbers in parentheses indicate the number of experiments done for each E_r obtained, plus or minus its standard deviation. The lower part shows the permeability coefficient ratios obtained from the E_r's using the appropriate Goldmann, Hodgkin, and Katz equation, as described in the Methods section.

*Calculated from the E_r obtained in Fig. 8 *A*.

DISCUSSION

In sea urchin sperm there is evidence for suspecting the participation of ionic channels in chemotaxis, the activation of motility and respiration, and the induction of the acrosome reaction by egg jelly (Schackmann et al., 1981; Christen et al., 1983; Lee and Garbers, 1986; García-Soto et al., 1987). During the acrosome reaction there are important changes in the plasma membrane permeability toward both monovalent and divalent cations. As a consequence, intracellular Ca^{2+} and pH increase and the membrane potential of the cell changes (Schackmann et al., 1981; García-Soto et al., 1987; González-Martínez and Darszon, 1987). The acrosome reaction and the events that accompany it are inhibited by Ca^{2+} (verapamil, dihydropyridines, La^{3+}) and K^+ (TEA^+, 4-aminopyridine) channel blockers (Darszon et al., 1988). These results clearly indicate that ionic channels, particularly for Ca^{2+} and K^+, play a key role in triggering this reaction.

Single-channel activity has been observed in whole sperm and sperm heads using the patch-clamp technique (Guerrero et al., 1987). However, a detailed analysis was precluded by the low rate of success in obtaining gigaseals displaying single-channel

activity. These findings emphasize the importance of a reconstitution approach to understand the role of ionic channels in cells as tiny as sperm (~2 μm in diameter) (in mammals see Young et al., 1988 and Cox and Peterson, 1989).

Previously the presence of four types of K^+ channels in sea urchin sperm was demonstrated in planar bilayers formed from monolayers derived from isolated sperm plasma membranes and liposomes at the tip of patch electrodes (Liévano et al., 1986). Because in these experiments, conducted mainly in the presence of monovalent cations, the pure lipid controls were free from channel-like artifacts, the first attempts to detect Ca^{2+} channels in this preparation were done using the same technique. Unfortunately, in many experiments it was observed that when the divalent cation concentration (Ba^{2+} or Ca^{2+}) was higher than 5 mM, the lipid bilayers made at the tip of patch-clamp electrodes always displayed a plethora of cationic single-channel–like artifacts in the absence of added protein. This behavior was consistently observed even with the purest lipid fractions (Avanti Polar Lipids, Inc., and lipids purified in the laboratory of the authors), and the purest reagents and water available, so this technique was abandoned. Subsequently, the Müller-Rudin technique for making planar bilayers was chosen because under our experimental conditions it did not produce artifacts.

This article demonstrates the existence of voltage-dependent and moderately Ca^{2+}-selective channels in the sea urchin sperm plasma membrane. The channels from isolated sea urchin sperm plasma membrane vesicles could be incorporated by fusion into planar lipid bilayers made both of bovine brain phospholipids (PE/PS 1:1) or from synthetic DiPhyPC. The lipid media did not have a significant effect on the conductance and behavior of the channel under the conditions tested. In 40 mM $Ba(HEPES)_2$, pH 8.0, PE/PS 1:1 bilayers, the γ_{MS} was 270 pS (Fig. 3 *B*), and in 50 mM $BaCl_2$, 10 mM HEPES-TMA, pH 8.0, DiPhyPC bilayers it was 266 pS (Fig. 5 *A*). These results suggest that the vestibules of the channel may be far from the interface, since there were only small conductance differences between charged and neutral bilayers. However, to establish this point, it will be necessary to compare conductance vs. divalent cation concentration curves with charged and neutral bilayers since the tested $BaCl_2$ concentrations could be saturating, as suggested by the linear *I-V* curve in asymmetrical solutions (200 mM *cis*/40 mM *trans*) (Bell and Miller, 1984). The channel γ_{MS} size in divalent cation solutions has the sequence $Ba^{2+} > Sr^{2+} > Ca^{2+}$, as in other types of Ca^{2+} channels (Hagiwara and Byerly, 1981; Tsien et al., 1987). This γ_{MS} conductance size sequence does not follow the sequence of ion mobilities, indicating that the ions must interact with the channel, which will be the subject of future work.

The ionic channels reported here have several uncommon characteristics: (*a*) their high conductance in divalent cation solutions, (*b*) several current levels and step sizes present at negative holding potentials, (*c*) the presence of only a main level of current at positive potentials, (*d*) their slightly higher selectivity toward divalent over monovalent cations, (*e*) the blocking of the channels by millimolar concentrations of Cd^{2+} and Co^{2+}, and (*f*) the permeability to Mg^{2+} in the *cis* side and its blocking effect when added in *trans*. All of these characteristics suggest that the Ca^{2+} channels detected in the sea urchin sperm plasma membrane are different from those usually present in other cells.

Ion channels poorly selective toward divalent cations have been described in mouse neurons (Nowack et al., 1984; MacDermont et al., 1986), in human neutrophils (Von Tscharner et al., 1986), and in rabbit arterial smooth muscle (Benham and Tsien, 1987), but they have a much smaller conductance and do not show a very complex kinetic behavior. There are also two examples of Ca^{2+} channels with high conductance and poor selectivity between divalent and monovalent ions in planar bilayer experiments: the Ca^{2+}-release channels from sarcoplasmic reticulum (Smith et al., 1985, 1986) and those from bovine brain microsomal membranes (Vassilev et al., 1987). The first has a P_{Ba}/P_{Cs} of 8, and the later P_{Ba}/P_{Cs} was 10.8. Recently it has been shown that the purified ryanodine receptor from rabbit skeletal muscle is the calcium-release channel from sarcoplasmic reticulum. At saturating $CaCl_2$ concentrations its main conductance was 172 pS and the channel displayed a $P_{Ca}/P_K = 6.6$ (Smith et al., 1988). These permeability coefficients are far from those reported for other types of calcium channels (Tsien et al., 1987) and are in the same order of magnitude of the ratios reported here for the sperm Ca^{2+} channels (see Table III). The ryanodine receptor channel is blocked by ruthenium red (~1 μM, Smith et al., 1988). In sea urchin sperm, both the egg jelly acrosome reaction and the associated $^{45}Ca^{2+}$ uptake are strongly inhibited by 50 μM of ruthenium red (unpublished results). Its effect, as well as that of ryanodine, remain to be evaluated on the sea urchin sperm Ca^{2+} channel to ascertain if there are more similitudes between the two channels.

To explain the voltage-dependent behavior and the unusual high conductance of the channel in divalent cation solutions, it could be thought of as a multipore complex having a concerted kinetic mechanism. At positive membrane potentials the channel remains in the γMS current level, while at negative potentials it is able to have random open-closed transitions to lesser conductance states, before inactivation (e.g., Fig. 1 *A*). The multipore complex must have a general gate, as suggested by the γMS open probability vs. E_m, which followed a Boltzmann function with an apparent gating charge of 3.9 and $E_{0.5}$ of -72 mV (Fig. 7). Since the probability of the open state has a substantial standard deviation, the gating charge value could lie between 2.5 and 4.5. The pores in the complex would have different conductances to explain the distinct current transition sizes observed (Figs. 2 *B*, 4 *C*, and 5 *C*), since apparently not all of them are multiples of a minimal value. In addition, the maximum conductance of the channel is several times smaller than the algebraic sum of the observed current states.

The idea of a multipore complex with a concerted kinetic mechanism would be consistent with the fact that the channels were always incorporated in the same way, irrespective of the cation used, as judged by the complex current pattern present in almost all the experiments (Figs. 1 *A*, 3 *A*, 4 *B*, and 5 *B*). In spite of the fact that the channel was incorporated with the same voltage dependence, its orientation in the planar bilayer is unknown. This makes it difficult to relate its characteristics to the physiology of the cell. Furthermore, we frequently obtained bilayers with more than one channel incorporated, and the maximal conductance corresponded to the sum of the γMS of the number of channels incorporated (e.g., Fig. 11). Since both the voltage-dependent anion channel from the outer membrane of mitochondria (VDAC), (a 32-kD dimer; Colombini, 1986), and the bacterial porins (trimers of ~35

kD polypeptides; Benz, 1986; Mauro et al., 1988) form channels with several subconductance states, the present Ca^{2+} channel could contain two or more pores in its structure. This idea seems plausible, since there are also some reports about Cl^- (Miller and White, 1984; Geletyuk and Kasachenko, 1985; Krouse et al., 1986), K^+ (Kasachenko and Geletyuk, 1984; Grygorczyk and Simon, 1986), and Ca^{2+} channels (Coyne et al., 1987), which appear to be formed from "protochannels," giving rise to a complex current pattern across the multimeric channels in response to their permeant ion driving force. Recently an anionic channel from amphibian skeletal muscle resembling the one discussed here was described (Woll et al., 1987; Woll and Neumcke, 1987).

Another possibility is that the channel has large vestibules and a short selectivity filter region like the maxi K^+ channel (see Yellen, 1987; Eisenmann and Dani, 1987). This would allow it to display selectivity among monovalent and divalent cations in spite of having a high conductance in divalent cation solutions. These two possibilities are not mutually exclusive, the channel could possess both of them. The authors are not aware of the existence of substate levels in the maxi Ca-K^+ channel, and in the sarcoplasmic reticulum K^+ channel only one substate is known (for a review, see Fox, 1987). In contrast, the sperm plasma membrane Ca^{2+} channel has up to nine current substate levels. This difference could indicate important structural differences.

At the moment it is difficult to know how the described sperm Ca^{2+} channels participate in the functioning of the cell. Two findings point to their possible involvement in the sperm acrosome reaction. Both Cd^{2+} (Fig. 10, Table I) and Co^{2+} (Fig. 11) block the channel at concentrations similar to those required to inhibit the acrosome reaction and the uptake of Ca^{2+} induced by egg jelly in sperm (Table II). On the other hand, verapamil and nisoldipine, which block certain types of Ca^{2+} channels and inhibit the acrosome reaction and Ca^{2+} uptake only when present before the addition of egg jelly, do not significantly modify the characteristics of the channel (not shown). Recently, evidence has been reported for the participation of two different Ca^{2+} channels in the triggering of the sea urchin sperm acrosome reaction (Guerrero and Darszon, 1989*a,b*). One is blocked by verapamil and nisoldipine and inactivates. The other is not blocked by these compounds, does not inactivate, allows Mn^{2+} to permeate and is blocked when sperm are exposed to seawater without Na^+, or with 40 mM KCl, or with 5 mM TEA^+, which are conditions that inhibit the acrosome reaction, but allow a transient increase in intracellular Ca^{2+}. These results suggest the possibility that the channel described here participates in the acrosome reaction and that it could be the one that allows the passage of Mn^{2+}.

Two experimental conditions known to induce the sea urchin sperm acrosome reaction in the absence of the egg jelly were used to increase the probability of finding activity: Mg^{2+}-free solutions (Collins and Epel, 1977) and an alkaline pH of 8.0 (Schackmann et al., 1981; García-Soto and Darszon, 1985) on both sides of the bilayers. It is possible that the experimental conditions used may influence the properties of the channel. As an example it can be mentioned that intracellular Mg^{2+} and pH have important effects on the kinetic and conduction behavior of some K^+ (Horie et al., 1987; Squire and Petersen, 1987; Golowasch, et al., 1986) and Ca^{2+}

channels (Nowack et al., 1984; Iljima et al., 1986; Konnert et al., 1987; Prod'hom et al., 1987; Pietrobon et al., 1988). In this regard, it was found that in solutions containing 10 mM $CaCl_2$ the channel was blocked by 50 mM $MgCl_2$ in *trans* at positive potentials, but when this salt was present in *cis*, Mg^{2+} permeated across the channel, with a P_{Ca}/P_{Mg} of 2.8 (Fig. 9 *A* and Table III). This vectorial effect of Mg^{2+} has also been documented for the Ca^{2+}-release channel from skeletal muscle sarcoplasmic reticulum (Smith et al., 1986), although in that channel, Mg^{2+} apparently blocks the channel by occluding the pore when present in *cis*. This finding could also be relevant for sperm physiology, since Mg^{2+} could act as a regulator for the sperm Ca^{2+} channels.

In the experiments with 50 mM divalent cation there were no current transitions to levels other than the main state at positive membrane potentials. Interestingly, in 10 mM $CaCl_2$ solutions, frequent transitions appeared at positive voltages between the main current level and a larger one. Thus, possibly there is another channel present with a conductance of ~50 pS that is blocked by higher Ca^{2+} concentrations and which will be further characterized in the future. This channel is voltage dependent, increasing its open probability as the voltage across the bilayer becomes more positive (see Fig. 9 *B*, records taken at positive E_m).

It should be mentioned that the plasma membranes used in this work were preferentially derived from the sperm flagella and have been shown to be quite pure (Cross, 1983; Darszon et al., 1984). The acrosome reaction occurs in the sperm head, thus it could be argued that the channels present in the flagellar plasma membrane are not involved in this reaction. It has been reported that there are differences in the composition of the flagellar and head sperm plasma membranes (García-Soto et al., 1988; Toowicharanont and Shapiro, 1988). However, both membrane fractions share components like the putative 210 kD egg jelly receptor (Trimmer et al., 1985) and high affinity sites for dihydropyridines (García-Soto et al., 1988) and verapamil (Toowicharanont and Shapiro, 1988). Also, they both respond in a similar fashion when exposed to egg jelly, increasing their uptake of $^{45}Ca^{2+}$ and $^{22}Na^{+}$ (Darszon et al., 1984; García-Soto et al., 1988). However, because during the mechanical separation of the flagella some heads are broken, it is not possible to rule out the possibility that the channel might be derived from the head, or even from the acrosomal membrane.

It has been postulated that egg jelly depolarizes sperm to induce the acrosome reaction (Schackmann et al., 1981). Recently it was shown that egg jelly triggers a K^{+}-dependent hyperpolarization that precedes the depolarization and is required for the acrosome reaction to occur (González-Martínez and Darszon, 1987). These results indicate that membrane potential changes, probably mediated by ionic channels, must occur for the acrosome reaction to happen. The channel described here is strongly voltage dependent, it inactivates at negative potentials and remains open at positive potentials. However, the physiological implications of this voltage dependence cannot be evaluated until its orientation in the planar bilayer is determined.

This work was partially supported by grants from the Consejo Nacional de Ciencia y Tecnología, the World Health Organization, project 87062, Special Program of Research Training in Human Reproduction, and the Organization of American States. A. Liévano had a doctoral fellowship from the Consejo Nacional de Ciencia y Technología.

The authors thank Irma Vargas and Lucia de De la Torre for their excellent technical assistance, M. Montes and J. Cortés for their help, and Dr. Armando Gómez-Puyou for critically reading the manuscript.

Original version received 10 November 1988 and accepted version received 28 June 1989.

REFERENCES

Bell, J., and C. Miller. 1984. Effects of phospholipid surface charge on ion conduction in the K^+ channel of sarcoplasmic reticulum. *Biophysical Journal.* 45:279–287.

Benham, C. D., and R. W. Tsien. 1987. A novel receptor-operated Ca^{2+}-permeable channel activated by ATP in smooth muscle. *Nature.* 328:275–278.

Benz, R. 1986. Analysis and chemical modification of bacterial porins. *In* Ion channel Reconstitution. Christopher Miller, editor. Plenum Publishing Corp., New York. 553–573.

Bezanilla, F. 1985. A high capacity data recording device based on a digital audio processor and a video cassette recorder. *Biophysical Journal.* 47:437–441.

Christen, R. R., R. W. Schackmann, and B. M. Shapiro. 1983. Metabolism of sea urchin sperm. Interrelationships between intracellular pH, ATPase activity and mitochondrial respiration. *Journal of Biological Chemistry.* 258:5392–5399.

Cohen, F. S., J. Zimmerberg, and A. Finkelstein. 1980. Fusion of phospholipid vesicles with planar phospholipid bilayer membranes. II. Incorporation of a vesicular membrane marker into the planar membrane. *Journal of General Physiology.* 75:241–250.

Collins, F., and D. Epel. 1977. The role of calcium ions in the acrosome reaction of sea urchin sperm. *Experimental Cell Research.* 106:211–222.

Colombini, M. 1986. Voltage gating in VDAC. Toward a molecular mechanism. *In* Ion Channel Reconstitution. Christopher Miller, editor. Plenum Publishing Corp., New York, pp. 533–552.

Cox, T., and R. N. Peterson. 1989. Identification of calcium conducting channels in isolated boar sperm plasma membranes. *Biochemical and Biophysical Research Communications.* 161:162–168.

Coyne, M. D., D. Dagan, and I. B. Levitan. 1987. Calcium and barium permeable channels from *Aplysia* nervous system reconstituted in lipid bilayers. *Journal of Membrane Biology.* 97:205–213.

Cross, N. L. 1983. Isolation and electrophoretic characterization of the plasma membrane of sea urchin sperm. *Journal of Cell Science.* 59:13–25.

Darszon, A., J. García-Soto, M. González, A. Guerrero, J. A. Sánchez, and A. Liévano. 1987. Ion transport mechanism in sea urchin sperm. *In* New Horizons in Sperm Cell Research. H. Mohri, editor. Japan Scientific Society Press, Tokyo/Gordon and Breach Scientific Publishers, New York, 169–183.

Darszon, A., M. Gould, L. de De Latorre, and I. Vargas. 1984. Response of isolated sperm plasma membranes from sea urchin to egg jelly. *European Journal of Biochemistry.* 144:515–522.

Darszon, A., A. Guerrero, A. Liévano, M. González-Martínez, and E. Morales. 1988. Ionic channels in sea urchin sperm physiology. *News in Physiological Sciences.* 3:181–185.

Domino, S. E., and D. L. Garbers. 1988. The fucose-sulfate glycoconjugate that induces an acrosome reaction in spermatozoa stimulates inositol 1,4,5-triphosphate accumulation. *Journal of Biological Chemistry.* 263:690–695.

Eisenman, G., and J. A. Dani. 1987. An introduction to molecular architecture and permeability of ion channels. *Annual Review of Biophysics and Biophysical Chemistry.* 16:205–226.

Fox, J. A. 1987. Ion channel subconductance states. *Journal of Membrane Biology.* 97:1–8.

Garbers, D. L., and J. G. Hardman. 1975. Factors released from sea urchin eggs affect cyclic nucleotide metabolism in sperm. *Nature.* 257:677–678.

García-Soto, J., and A. Darszon. 1985. High pH-induced acrosome reaction and Ca^{2+} uptake in sea urchin sperm suspended in Na^+-free sea water. *Developmental Biology.* 110:338–345.

García-Soto, J., M. González-Martínez, L. de De la Torre, and A. Darszon. 1987. Internal pH can regulate Ca^{2+} uptake and the acrosome reaction in sea urchin sperm. *Developmental Biology.* 120:112–120.

García-Soto, J., M. Mourelle, I. Vargas, L. de De la Torre, E. Ramirez, A. M. Lopez-Colomé, and A. Darszon. 1988. Sea urchin sperm head plasma membranes: characteristics and egg-jelly induced Ca^{2+} and Na^{+} uptake. *Biochimica et Biophysica Acta.* 944:1–12.

Geletyuk, V. I., and V. N. Kasachenko. 1985. Single Cl-channels in molluscan neurons: multiplicity of the conductance states. *Journal of Membrane Biology.* 86:9–15.

Golowasch, J., A. Kirkwood, and C. Miller. 1986. Allosteric effects of Mg^{2+} on the gating of Ca^{2+}-activated K^{+} channels from mammalian skeletal muscle. *Journal of Experimental Biology.* 124:5–13.

González-Martínez, M., and A. Darszon. 1987. A fast transient hyperpolarization occurs during the sea urchin sperm acrosome reaction induced by egg jelly. *FEBS Letters.* 218:247–250.

Grygorczyk, R., and M. Simon. 1986. Single K^{+} channels in the apical membrane of amphibian peritoneum. *Biochimica et Biophysica Acta.* 861:365–368.

Guerrero, A., and A. Darszon. 1989*a*. Evidence for the activation of two different Ca^{2+} channels during the egg jelly–induced acrosome reaction of sea urchin sperm. *Journal of Biological Chemistry.* 264:19593–19599.

Guerrero, A., and A. Darszon. 1989*b*. Egg jelly triggers a calcium influx which inactivates and is inhibited by calmodulin antagonists in the sea urchin sperm. *Biochimica et Biophysica Acta.* 980:109–116.

Guerrero, A., J. A. Sánchez, and A. Darszon. 1987. Single-channel activity in sea urchin sperm revealed by the patch-clamp technique. *FEBS Letters.* 220:295–298.

Hagiwara, S., and L. Byerly. 1981. Calcium channel. *Annual Review of Neurosciences.* 4:69–125.

Harned, H. S., and B. B. Owen. 1958. The Physical Chemistry of Electrolytic Solutions. Reinhold Book Co., New York. 803 pp.

Hartshorne, R., M. Tamkum, and M. Montal. 1986. The reconstituted sodium channel from brain. *In* Ion Channel Reconstitution. Christopher Miller, editor. Plenum Publishing Corp., New York. 337–362.

Horie, M., H. Irisawa, and A. Noma. 1987. Voltage-dependent magnesium block of adenosine-triphosphate-sensitive potassium channel in guinea-pig ventricular cells. *Journal of Physiology.* 387:251–272.

Iljima, T., S. Ciani, and S. Hagiwara. 1986. Effects of the external pH on Ca channels: experimental studies and theoretical considerations using a two site, two ion model. *Proceedings of the National Academy of Sciences.* 83:654–658.

Kasachenko, V. N., and V. I. Geletyuk. 1984. The potential-dependent K^{+} channel in molluscan neurons is organized in a cluster of elementary channels. *Biochimica et Biophysica Acta.* 773:132–142.

Kazazoglou, T., R. W. Schackmann, M. Fosset, and B. M. Shapiro. 1985. Calcium channel antagonists inhibit the acrosome reaction and bind to plasma membranes of sea urchin sperm. *Proceedings of the National Academy of Sciences.* 82:1460–1464.

Konnert, A., H. D. Lux, and M. Morad. 1987. Proton-induced transformation of calcium channel in chick dorsal root ganglion cells. *Journal of Physiology.* 386:603–633.

Kopf, G. S., and D. L. Garbers. 1980. Calcium and fucose-sulfate-rich polymer regulate sperm cyclic nucleotide metabolism and the acrosome reaction. *Biology of Reproduction.* 22:1118–1126.

Krouse, M. E., G. T. Tschneider, and P. W. Gage. 1986. A large anion channel has seven conductance levels. *Nature.* 319:58–60.

Lee, H. C. 1984. A membrane potential-sensitive Na^+-H^+ exchange system in flagella isolated from sea urchin spermatozoa. *Journal of Biological Chemistry.* 259:15315–15319.

Lee, H. C. 1985. The voltage-sensitive Na^+/H^+ exchange in sea urchin spermatozoa flagellar membrane vesicles studied with an entrapped pH probe. *Journal of Biological Chemistry.* 260:10794–10799.

Lee, H. C., and D. L. Garbers. 1986. Modulation of the voltage-sensitive Na^+/H^+ exchange in sea urchin spermatozoa through membrane potential changes induced by the egg peptide speract. *Journal of Biological Chemistry.* 261:16026–16032.

Liévano, A., J. A. Sánchez, and A. Darszon. 1986. Single channel activity of bilayers derived from sea urchin sperm plasma membranes at the tip of a patch-clamp electrode. *Developmental Biology.* 112:253–257.

Liévano, A., E. Vega, L. de De La Torre, I. Vargas, and A. Darszon. 1988. Ca^{2+} channels from the sea urchin sperm plasma membranes incorporated into planar bilayers. *Biophysical Journal.* 54:559*a*. (Abstr.)

MacDermont, A. B., M. L. Mayer, G. L. Westbrook, S. J. Smith, and J. L. Barker. 1986. NMDA receptor activation increases cytoplasmic calcium concentration in cultured spinal chord neurons. *Nature.* 321:519–522.

Mauro, A., M. Blake, and P. Labarca. 1988. Voltage gating of conductance in lipid bilayers induced by porin from outer membrane from *Neisseriae gonorrhoeae. Proceedings of the National Academy of Sciences.* 85:1071–1075.

Miller, C., and E. Racker. 1976. Ca^{2+} induced fusion of fragmented sarcoplasmic reticulum with artificial planar bilayers. *Journal of Membrane Biology.* 30:283–300.

Miller, C., and M. M. White. 1984. Dimeric structure of single chloride channels from torpedo electroplax. *Proceedings of the National Academy of Sciences.* 81:2772–2775.

Müller, P., and D. O. Rudin. 1969. Bimolecular lipid membranes: techniques of formation, study of electrical properties, and induction of gating phenomena. *In* Laboratory Techniques in Membrane Biophysics. H. De Passow and R. Stampfli, editors. Springer-Verlag, Berlin, 141–156.

Nowack, L., P. Bregestovski, P. Ascher, A. Herbert, and A. Prochiantz. 1984. Magnesium gates glutamate-activated channels in mouse central neurons. *Nature.* 307:462–465.

Pietrobon, D., B. Prod'hom, and P. Hess. 1988. Conformational changes associated with ion permeation in L-type calcium channels. *Nature.* 333:373–376.

Prod'hom, B., D. Pietrobon, and P. Hess. 1987. Direct measurement of proton transfer rates to a group controlling the dihydropyridine-sensitive Ca^{2+} channel. *Nature.* 329:243–246.

Schackmann, R. W., R. Christen, and B. M. Shapiro. 1981. Membrane potential depolarization and increased intracellular pH accompany the acrosome reaction of sea urchin sperm. *Proceedings of the National Academy of Sciences.* 78:6066–6070.

Schackmann, R. W., E. M. Eddy, and B. M. Shapiro, 1978. The acrosome reaction of *Strongylocentrotus purpuratus* sperm. Ion requirements and movements. *Developmental Biology.* 65:483–495.

Schackmann, R. W., and B. M. Shapiro. 1981. A partial sequence of ionic changes associated with the acrosome reaction of *Strongylocentrotus purpuratus. Developmental Biology.* 81:145–154.

Smith, J. S., R. Coronado, and G. Meissner. 1985. Sarcoplasmic reticulum contains adenine nucleotide-activated calcium channels. *Nature.* 316:446–449.

Smith, J. S., R. Coronado, and G. Meissner. 1986. Single channel measurements of the calcium release channel from skeletal muscle sarcoplasmic reticulum. *Journal of General Physiology.* 88:573–588.

Smith, J. S., T. Imagawa, J. Ma, M. Fill, K. P. Campbell, and R. Coronado. 1988. Purified ryanodine receptor from rabbit skeletal muscle is the calcium-release channel of sarcoplasmic reticulum. *Journal of General Physiology.* 92:1–26.

Squire, L. G., and O. H. Petersen. 1987. Modulation of Ca^{2+}- and voltage-activated K^+ channels by internal Mg^{2+} in salivary acinar cells. *Biochimica et Biophysica Acta.* 899:171–175.

Toowicharanont, P., and B. M. Shapiro. 1988. Regional differentiation of sea urchin sperm plasma membrane: enzyme activities and D600 binding sites. *Journal of Biological Chemistry.* 263:6877–6883.

Trimmer, J. S., I. S. Trowbridge, and V. D. Vacquier. 1985. Monoclonal antibody to a membrane glycoprotein inhibits the acrosome reaction and associated Ca^{2+} and H^+ fluxes of sea urchin sperm. Cell. 40:697–703.

Tsien, R. W., P. Hess, E. W. McCleskey, and R. L. Rosemberg. 1987. Calcium channels: Mechanisms of selectivity, permeation and block. *Annual Review of Biophysics and Biophysical Chemistry.* 16:265–290.

Vassilev, P. M., M. P. Kanazisska, and H. T. Tien. 1987. Ca^{2+} channels from brain microsomal membranes reconstituted in patch-clamped bilayers. *Biochimica et Biophysica Acta.* 897:324–330.

Von Tscharner, V., B Prod'hom, M. Maggiolini, and H. Reuter. 1986. Ion channels in human neutrophils activated by a rise in free cytosolic calcium concentration. *Nature.* 324:369–372.

Woll, K. H., M. D. Leivowitz, B. Neumcke, and B. Hille. 1987. A high conductance anion channel in adult amphibian skeletal muscle. *Pflügers Archiv.* 410:632–640.

Woll, K. H., and B. Neumcke. 1987. Conductance properties and voltage-dependence of an anion channel in amphibian skeletal muscle. *Pflügers Archiv.* 410:641–647.

Yellen, G. 1987. Permeation in potassium channels: implications for channel structure. *Annual Review of Biophysics and Biophysical Chemistry.* 16:227–246.

Young, G. P. H., S. S. Koide, M. Goldstein, and J. D. E. Young. 1988. Isolation and partial characterization of an ion channel protein from human sperm membranes. *Archives of Biochemistry and Biophysics.* 262:491–500.